Synthesis and Characterization of Luminescent Rhenium(I)−Platinum(II) Polypyridine Bichromophoric Alkynyl-Bridged Molecular Rods

Sally Chan-Fung Lam, Vivian Wing-Wah Yam,* Keith Man-Chung Wong,* Eddie Chung-Chin Cheng, and Nianyong Zhu

Centre for Carbon-Rich Molecular and Nano-Scale Metal-Based Materials Research, Department of Chemistry, The University of Hong Kong, Pokfulam Road, Hong Kong SAR, People's Republic of China

Received April 14, 2005

The first class of luminescent heterobimetallic rhenium(I)−platinum(II) polypyridine alkynyl complexes, $[(N\hat{}N)(CO)_3Re\{C{\equiv}C-(C_6H_4)_n-C{\equiv}C\}Pt(N\hat{}N\hat{}N)]OTf$ ($N\hat{}N$ = bpy, $^tBu_2$-bpy, $(CF_3)_2$bpy, NO_2phen; $N\hat{}N\hat{}N$ = tpy, $^tBu_3$tpy; $n = 0, 1$), has been successfully synthesized. The X-ray crystal structures of $[(bpy)(CO)_3Re\{C{\equiv}C-C_6H_4-C{\equiv}C\}Pt(^tBu_3tpy)]OTf$ (**1**) and $[(NO_2phen)(CO)_3Re\{C{\equiv}C-C_6H_4-C{\equiv}C\}Pt(^tBu_3tpy)]OTf$ (**4**) have been determined. Their photophysical and electrochemical behavior have also been studied and discussed. An unexpected localization of the lowest-energy emissive state on the platinum(II) terpyridyl moiety in these heterometallic bichromophoric systems was observed.

Introduction

In recent years, the chemistry of metal-containing alkynyls has captured the attention of many researchers due to their rigid structures as well as the rich spectroscopic and photophysical behavior associated with some of these complexes.[1] Complexes of rhenium alkynyls are known, but with most of the studies concentrated on the homometallic systems.[2] Gladysz and coworkers reported a series of alkynyl-bridged dinuclear rhenium(I) alkynyls, including one that involved 20 carbon atoms in the chain spanning two redox-active $[Re(\eta^5\text{-}C_5Me_5)(NO)(PPh_3)]$ moieties.[2a] Examples of heteronuclear rhenium alkynyl rods are scarce,[3] and most of them were confined to the study of their structural and electrochemical properties. An example is the work of Gladysz and Lapinte, which focuses on the synthesis and redox behavior of a heterobimetallic butadiynediyl complex, $[(\eta^5\text{-}C_5Me_5)Re(NO)(PPh_3)(C{\equiv}C-C{\equiv}C)(dppe)\text{-}Fe(\eta^5\text{-}C_5Me_5)]$.[4] With our recent interest in incorporating metal-to-ligand charge transfer (MLCT) luminophores of rhenium(I) diimine and platinum(II) terpyridine systems into alkynyl systems to generate luminescent metal-containing alkynyls,[5,6] as well as our recent efforts in utilizing the rhenium(I) diimine alkynyl moieties to serve as versatile and powerful building blocks for the assembly of various luminescent mixed-metal carbon-rich molecular rods of rhenium(I)−iron(II),[7a] −gold(I),[7b] −silver(I),[7c,d,g] −copper(I),[7d,g] −cobalt(II),[7e]

* Corresponding authors. E-mail: wwyam@hku.hk; wongmc@hku.hk.

(1) (a) Beck, W.; Niemer, B.; Wieser, M. *Angew. Chem., Int. Ed. Engl.* **1993**, *32*, 923. (b) Narvor, N. L.; Toupet, L.; Lapinte, C. *J. Am. Chem. Soc.* **1995**, *117*, 7129. (c) Bruce, M. I.; Low, P. J.; Costuas, K.; Halet, J. F.; Best, S. P.; Heath, G. A. *J. Am. Chem. Soc.* **2000**, *122*, 1949. (d) Xu, G. L.; Zou, G.; Ni, Y. H.; DeRosa, M. C.; Crutchley, R. J.; Ren, T. *J. Am. Chem. Soc.* **2003**, *125*, 10057. (e) Long, N. J.; Williams, C. K. *Angew. Chem., Int. Ed.* **2003**, *42*, 2586. (f) Szafert, S.; Gladysz, J. A. *Chem. Rev.* **2003**, *103*, 4175.

(2) (a) Dembinski, R.; Bartik, T.; Bartik, B.; Jaeger, M.; Gladysz, J. A. *J. Am. Chem. Soc.* **2000**, *122*, 810. (b) Meyer, W. E.; Amoroso, A. J.; Horn, C. R.; Jaeger, M.; Gladysz, J. A. *Organometallics* **2001**, *20*, 1115. (c) Horn, C. R.; Martín-Alvarez, J. M.; Gladysz, J. A. *Organometallics* **2002**, *21*, 5386. (d) Horn, C. R.; Gladysz, J. A. *Eur. J. Inorg. Chem.* **2003**, 2211.

(3) (a) Weidmann, T.; Weinrich, V.; Wagner, B.; Robl, C.; Beck, W. *Chem. Ber.* **1991**, *124*, 1363. (b) Weng, W.; Bartik, T.; Brady, M.; Bartik, B.; Ramsden, J. A.; Arif, A. M.; Gladysz, J. A. *J. Am. Chem. Soc.* **1995**, *117*, 11922. (c) Falloon, S. B.; Arif, A. M.; Gladysz, J. A. *Chem. Commun.* **1997**, 629. (d) Falloon, S. B.; Weng, W.; Arif, A. M.; Gladysz, J. A. *Organometallics* **1997**, *16*, 2008. (e) Bartik, T.; Weng, W.; Ramsden, J. A.; Szafert, S.; Falloon, S. B.; Arif, A. M.; Gladysz, J. A. *J. Am. Chem. Soc.* **1998**, *120*, 11071. (f) Falloon, S. B.; Szafert, S.; Arif, A. M.; Gladysz, J. A. *Chem. Eur. J.* **1998**, *4*, 1033. (g) Kühn, F. E.; Zuo, J. L.; de Biani, F. F.; Santos, A. M.; Zhang, Y.; Zhao, J.; Sandulache, A.; Herdtweck, E. *New J. Chem.* **2004**, *28*, 43.

(4) (a) Paul, F.; Meyer, W. E.; Toupet, L.; Jiao, H.; Gladysz, J. A.; Lapinte, C. *J. Am. Chem. Soc.* **2000**, *122*, 9405. (b) Jiao, H.; Costuas, K.; Gladysz, J. A.; Halet, J. F.; Guillemot, M.; Toupet, L.; Paul, F.; Lapinte, C. *J. Am. Chem. Soc.* **2003**, *125*, 9511.

(5) (a) Yam, V. W. W.; Lau, V. C. Y.; Cheung, K. K. *Organometallics* **1995**, *14*, 2749. (b) Yam, V. W. W.; Lau, V. C. Y.; Cheung, K. K. *Organometallics* **1996**, *15*, 1740. (c) Yam, V. W. W.; Chong, S. H. F.; Cheung, K. K. *Chem. Commun.* **1998**, 2121. (d) Yam, V. W. W.; Lo, K. K. W.; Wong, K. M. C. *J. Organomet. Chem*. **1999**, *578*, 3. (e) Yam, V. W. W.; Chong, S. H. F.; Ko, C. C.; Cheung, K. K. *Organometallics* **2000**, *19*, 5092. (f) Yam, V. W. W. *Chem. Commun* **2001**, 789. (g) Yam, V. W. W.; Wong, K. M. C.; Chong, S. H. F.; Lau, V. C. Y.; Lam, S. C. F.; Zhang, L.; Cheung, K. K. *J. Organomet. Chem*. **2003**, *670*, 205.

(6) (a) Yam, V. W. W.; Tang, R. P. L.; Wong, K. M. C.; Cheung, K. K. *Organometallics* **2001**, *20*, 4476. (b) Hui, C. K.; Chu, B. W. K.; Zhu, N.; Yam, V. W. W. *Inorg. Chem.* **2002**, *41*, 6178. (c) Yam, V. W. W.; Wong, K. M. C.; Zhu, N. *J. Am. Chem. Soc.* **2002**, *124*, 6506. (d) Yam, V. W. W.; Wong, K. M. C.; Zhu, N. *Angew. Chem., Int. Ed.* **2003**, *42*, 1400. (e) Tao, C. H.; Wong, K. M. C.; Zhu, N.; Yam, V. W. W. *New J. Chem.* **2003**, *27*, 150. (f) Yu, C.; Wong, K. M. C.; Chan, K. H. Y.; Yam, V. W. W. *Angew. Chem., Int. Ed.* **2005**, *44*, 791. (g) Wong, K. M. C.; Tang, W. S.; Lu, X. X.; Zhu, N.; Yam, V. W. W. *Inorg. Chem.* **2005**, *44*, 1492. (h) Yam, V. W. W.; Chan, K. H. Y.; Wong, K. M. C.; Zhu, N. *Chem. Eur. J.* **2005**, *11*, 4535.

(7) (a) Wong, K. M. C.; Lam, S. C. F.; Ko, C. C.; Zhu, N.; Yam, V. W. W.; Roué, S.; Lapinte, C.; Fathallah, S.; Costuas, K.; Kahlal, S.; Halet, J. F. *Inorg. Chem.* **2003**, *42*, 7086. (b) Cheung, K. L.; Yip, S. K.; Yam, V. W. W. *J. Organomet. Chem.* **2004**, *689*, 4451.; (c) Yam, V. W. W.; Lo, W. Y.; Zhu, N. *Chem. Commun*. **2003**, 2446. (d) Yam, V. W. W.; Lo, W. Y.; Lam, C. H.; Fung, W. K. M.; Wong, K. M. C.; Lau, V. C. Y.; Zhu, N. *Coord. Chem. Rev.* **2003**, *245*, 39. (e). Chong, S. H. F.; Lam, S. C. F.; Ko, C. C.; Yam, V. W. W. *J. Cluster Sci.* **2004**, *15*, 301. (f) Chong, S. H. F.; Lam, S. C. F.; Yam, V. W. W.; Zhu, N.; Cheung, K. K.; Fathallah, S.; Costuas, K.; Halet, J. F. *Organometallics* **2004**, *23*, 4924. (g) Yam, V. W. W. *J. Organomet. Chem.* **2004**, *689*, 1393.

10.1021/om0502887 CCC: $30.25
Publication on Web 07/19/2005

Scheme 1. Synthetic Scheme of the Heterobimetallic Rhenium(I)−Platinum(II) Alkynyl Complexes

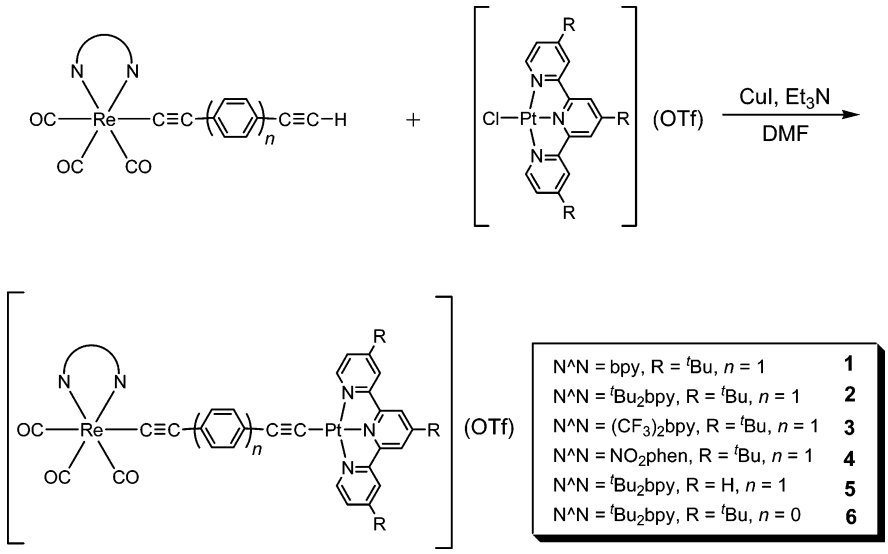

and −palladium(II),[7f] a program was initiated to investigate the possible incorporation of the platinum(II) terpyridyl unit into the rhenium(I) alkynyl systems. It is envisaged that their luminescence properties would be perturbed or varied via the connecting of the two different luminophoric units through the alkynyl bridge. Herein is described the first report on the isolation, characterization, and X-ray crystal structures of a new class of luminescent heterobimetallic Re(I)−Pt(II) complexes, [(N^N)(CO)$_3$Re{C≡C−(C$_6$H$_4$)$_n$−C≡C}Pt(N^N^N)]OTf (N^N = bpy, ^{t}Bu$_2$bpy, (CF$_3$)$_2$bpy, NO$_2$phen; N^N^N = tpy, ^{t}Bu$_3$tpy; n = 0, 1) (Scheme 1). Their electronic absorption, luminescence, and electrochemical properties have also been studied, and their assignments were supported by extended Hückel molecular orbital (EHMO) studies.

Experimental Section

Materials and Reagents. The rhenium alkynyl precursors, [Re(N^N)(CO)$_3$(C≡C−C$_6$H$_4$−C≡CH)][8] and [Re(^{t}Bu$_2$bpy)(CO)$_3$(C≡C−C≡CH)],[5c] together with the platinum terpyridyl precursors, [Pt(N^N^N)Cl]OTf,[9] were synthesized according to the literature procedures. Copper(I) iodide was purchased from Aldrich Chemical Co. Triethylamine was purchased from Lancaster Synthesis Ltd. All solvents were purified and distilled using standard procedures before use.[10] All other reagents were of analytical grade and were used as received.

Syntheses. All reactions were performed under anaerobic and anhydrous conditions using standard Schlenk techniques under an inert atmosphere of nitrogen.

[(bpy)(CO)$_3$Re(C≡C−C$_6$H$_4$−C≡C)Pt(^{t}Bu$_3$tpy)]OTf (1). A DMF solution (5 mL) of [Re(bpy)(CO)$_3$(C≡C−C$_6$H$_4$−C≡CH)] (106 mg, 0.19 mmol) was added into a DMF solution (5 mL) containing [Pt(^{t}Bu$_3$tpy)Cl]OTf (100 mg, 0.13 mmol), CuI (2.7 mg, 0.01 mmol), and Et$_3$N (4 mL). The reaction mixture was allowed to stir at room temperature for 24 h, after which addition of diethyl ether caused precipitation. The red precipitate was collected and purified by column chromatography on silica gel using dichloromethane−acetone (4:1 v/v) as eluent, followed by subsequent recrystallization from either acetonitrile−diethyl ether or dichloromethane−diethyl ether to afford **1** as deep red crystals. Yield: 62 mg, 37%. ^{1}H NMR (400 MHz, CD$_3$CN, 298 K, δ/ppm): δ 1.45 (s, 18H, ^{t}Bu), 1.53 (s, 9H, ^{t}Bu), 6.79 (d, 2H, J = 7.7 Hz, −C$_6$H$_4$−), 7.16 (d, 2H, J = 7.7 Hz, −C$_6$H$_4$−), 7.64 (ddd, 2H, J = 1.0, 6.1, and 8.2 Hz, 4- and 4′-bipyridyl H's), 7.71 (dd, 2H, J = 2.0 and 6.1 Hz, tpy), 8.20 (ddd, 2H, J = 1.5, 5.6, and 8.2 Hz, 5- and 5′-bipyridyl H's), 8.27 (d, 2H, J = 2.0 Hz, tpy), 8.31 (s, 2H, tpy), 8.47 (dd, 2H, J = 1.5 and 6.1 Hz, 3- and 3′-bipyridyl H's), 8.98 (d, 2H, J = 6.1 Hz, tpy), 9.08 (dd, 2H, J = 1.0 and 5.6 Hz, 6- and 6′-bipyridyl H's). Positive FAB-MS: ion clusters at m/z 1148 {M}$^+$, 1120 {M − CO}$^+$. IR (KBr disk, ν/cm^{-1}): 1885 (s), 1906 (s), 2004 (s) ν(C≡O); 2089 (w), 2113 (w) ν(C≡C). Anal. Found (%): C 45.25, H 3.77, N 5.11. Calcd for [(bpy)(CO)$_3$Re(C≡C−C$_6$H$_4$−C≡C)Pt(^{t}Bu$_3$tpy)]OTf·CH$_2$Cl$_2$: C 45.22, H 3.58, N 5.07.

[(^{t}Bu$_2$bpy)(CO)$_3$Re(C≡C−C$_6$H$_4$−C≡C)Pt(^{t}Bu$_3$tpy)]OTf (2). The procedure was similar to that described for the preparation of **1**, except [Re(^{t}Bu$_2$bpy)(CO)$_3$(C≡C−C$_6$H$_4$−C≡CH)] (127 mg, 0.19 mmol) was used in place of [Re(bpy)(CO)$_3$(C≡C−C$_6$H$_4$−C≡CH)] to give red crystals of **2**. Yield: 56 mg, 31%. ^{1}H NMR (300 MHz, CD$_3$CN, 298 K, δ/ppm): δ 1.47 (s, 18H, ^{t}Bu), 1.49 (s, 18H, ^{t}Bu), 1.54 (s, 9H, ^{t}Bu), 6.78 (d, 2H, J = 7.7 Hz, −C$_6$H$_4$−), 7.17 (d, 2H, J = 7.7 Hz, −C$_6$H$_4$−), 7.65 (dd, 2H, J = 1.9 and 5.9 Hz, 5- and 5′-bipyridyl H's), 7.72 (dd, 2H, J = 1.9 and 5.9 Hz, tpy), 8.29 (d, 2H, J = 1.9 Hz, tpy), 8.33 (s, 2H, tpy), 8.46 (d, 2H, J = 1.9 Hz, 3- and 3′-bipyridyl H's), 8.95 (d, 2H, J = 5.9 Hz, tpy), 9.01 (d, 2H, J = 5.9 Hz, 6- and 6′-bipyridyl H's). Positive FAB-MS: ion clusters at m/z 1258 {M}$^+$, 1230 {M − CO}$^+$. IR (KBr disk, ν/cm^{-1}): 1884 (s), 1902 (s), 2003 (s) ν(C≡O); 2088 (w), 2114 (w) ν(C≡C). Anal. Found (%): C 48.79, H 4.44, N 4.77. Calcd for [(^{t}Bu$_2$bpy)(CO)$_3$Re(C≡C−C$_6$H$_4$−C≡C)Pt(^{t}Bu$_3$tpy)]OTf·$^2/_3$CH$_2$Cl$_2$: C 48.98, H 4.57, N 4.79.

[{(CF$_3$)$_2$bpy}(CO)$_3$Re(C≡C−C$_6$H$_4$−C≡C)Pt(^{t}Bu$_3$tpy)]OTf (3). The procedure was similar to that described for the preparation of **1**, except [Re{(CF$_3$)$_2$bpy}(CO)$_3$(C≡C−C$_6$H$_4$−C≡CH)] (127 mg, 0.19 mmol) was used in place of [Re(bpy)(CO)$_3$(C≡C−C$_6$H$_4$−C≡CH)] to give red crystals of **3**. Yield: 55 mg, 30%. ^{1}H NMR (300 MHz, CD$_3$CN, 298 K, δ/ppm): δ 1.43 (s, 18H, ^{t}Bu), 1.49 (s, 9H, ^{t}Bu), 6.76 (d, 2H, J = 7.7 Hz, −C$_6$H$_4$−), 7.12 (d, 2H, J = 7.7 Hz, −C$_6$H$_4$−), 7.65 (dd, 2H, J = 1.9 and 5.8 Hz, 5- and 5′-bipyridyl H's), 7.88 (dd, 2H, J = 1.9 and 5.9 Hz, tpy), 8.20 (d, 2H, J = 1.9 Hz, tpy), 8.26 (s, 2H, tpy), 8.85 (d, 2H, J = 5.9 Hz, tpy), 8.90 (d, 2H, J = 1.9 Hz, 3- and 3′-bipyridyl H's), 9.28 (d, 2H, J = 5.8 Hz, 6- and 6′-bipyrdyl H's). Positive FAB-MS: ion clusters at m/z 1282 {M}$^+$, 1254 {M − CO}$^+$. IR (KBr disk, ν/cm^{-1}): 1890 (s), 1919 (s), 2011 (s) ν(C≡

(8) Wong, K. M. C. Ph.D. Thesis, The University of Hong Kong, 1998.
(9) (a) Yip, H. K.; Cheng, L. K.; Cheung, K. K.; Che, C. M. *Inorg. Chem.* **1993**, *19*, 2933. (b) Buechner, R.; Field, J. S.; Haines, R. J.; Cunningham, C. T.; McMillin, D. R. *Inorg. Chem.* **1997**, *36*, 3952.
(10) Perrin, D. D.; Armarego, W. L. F. *Purification of Laboratory Chemicals*, 3rd ed.; Pergamon: Oxford, U.K., 1988.

O); 2088 (w), 2111 (w) ν(C≡C). Anal. Found (%): C 41.51, H 3.03, N 4.56. Calcd for [{$(CF_3)_2$bpy}$(CO)_3$Re(C≡C−C_6H_4−C≡C)Pt(^{t}Bu_3tpy)]OTf·$2CH_2Cl_2$: C 41.23, H 3.08, N 4.37.

[$(NO_2$phen)$(CO)_3$Re(C≡C−C_6H_4−C≡C)Pt(^{t}Bu_3tpy)]OTf (4). The procedure was similar to that described for the preparation of **1**, except [Re$(NO_2$phen$)(CO)_3$(C≡C−C_6H_4−C≡CH)] (102 mg, 0.19 mmol) was used in place of [Re(bpy)$(CO)_3$(C≡C−C_6H_4−C≡CH)] to give red crystals of **4**. Yield: 58 mg, 38%. ^{1}H NMR (300 MHz, CD_3CN, 298 K, δ/ppm): δ 1.48 (s, 18H, ^{t}Bu), 1.49 (s, 9H, ^{t}Bu), 6.58 (d, 2H, J = 8.0 Hz, −C_6H_4−), 7.03 (d, 2H, J = 8.0 Hz, −C_6H_4−), 7.91 (dd, 2H, J = 2.0 and 5.9 Hz, tpy), 8.31 (m, 2H, 3- and 8-phen H's), 8.69 (d, 2H, J = 2.0 Hz, tpy), 8.74 (s, 2H, tpy), 9.13 (d, 2H, J = 5.9 Hz, tpy), 9.22 (d, 1H, J = 1.2 Hz, 7-phen H), 9.34 (s, 1H, 6-phen H), 9.41 (d, 1H, J = 1.2 Hz, 4-phen H), 9.71 (m, 2H, 2 and 9-phen H's). Positive FAB-MS: ion clusters at *m/z* 1216 {M}$^+$, 1188 {M − CO}$^+$. IR (KBr disk, ν/cm^{-1}): 1891 (s), 1912 (s), 2008 (s) ν(C≡O); 2088 (w), 2113 (w) ν(C≡C). Anal. Found (%): C 46.05, H 3.46, N 6.21. Calcd for [$(NO_2$phen$)(CO)_3$Re(C≡C−C_6H_4−C≡C)Pt(^{t}Bu_3tpy)]OTf·$^1/_4CH_2Cl_2$: C 46.13, H 3.38, N 6.06.

[(^{t}Bu_2bpy)$(CO)_3$Re(C≡C−C_6H_4−C≡C)Pt(tpy)]OTf (5). The procedure was similar to that described for the preparation of **1**, except [Pt(tpy)Cl]OTf (80 mg, 0.13 mmol) was used in place of [Pt(^{t}Bu_3tpy)Cl]OTf to give red crystals of **5**. Yield: 57 mg, 35%. ^{1}H NMR (300 MHz, CD_3CN, 298 K, δ/ppm): δ 1.49 (s, 18H, ^{t}Bu), 6.83 (d, 2H, J = 7.9 Hz, −C_6H_4−), 7.06 (d, 2H, J = 7.9 Hz, −C_6H_4−), 7.61 (t, 2H, J = 6.1 Hz, tpy), 7.65 (dd, 2H, J = 1.8 and 5.9 Hz, 5- and 5′-bipyridyl H's), 8.05 (m, 4H, tpy), 8.21 (m, 3H, tpy), 8.44 (d, 2H, J = 1.8 Hz, 3- and 3′-bipyridyl H's,), 8.83 (d, 2H, J = 4.8 Hz, tpy), 8.95 (d, 2H, J = 5.9 Hz, 6- and 6′-bipyridyl H's). Positive FAB-MS: ion clusters at *m/z* 1090 {M}$^+$, 1062 {M − CO}$^+$. IR (KBr disk, ν/cm^{-1}): 1886 (s), 1904 (s), 2003 (s) ν(C≡O); 2087 (w), 2117 (w) ν(C≡C). Anal. Found (%): C 41.62, H 2.97, N 5.23. Calcd for [(^{t}Bu_2bpy)$(CO)_3$Re(C≡C−C_6H_4−C≡C)Pt(tpy)]OTf·$2CH_2Cl_2$: C 41.70, H 3.05, N 4.96.

[(^{t}Bu_2bpy)$(CO)_3$Re(C≡C−C≡C)Pt(^{t}Bu_3tpy)]OTf (6). The procedure was similar to that described for the preparation of **1**, except [Re(^{t}Bu_2bpy)$(CO)_3$(C≡C−C≡CH)] (114 mg, 0.19 mmol) was used in place of [Re(bpy)$(CO)_3$(C≡C−C_6H_4−C≡CH)] to give red crystals of **6**. Yield: 52 mg, 30%. ^{1}H NMR (300 MHz, CD_3CN, 298 K, δ/ppm): δ 1.40 (s, 18H, ^{t}Bu), 1.47 (s, 18H, ^{t}Bu), 1.48 (s, 9H, ^{t}Bu), 7.56 (dd, 2H, J = 1.9 and 5.9 Hz, 5- and 5′-bipyridyl H's), 7.66 (dd, 2H, J = 1.9 and 5.9 Hz, tpy), 8.13 (d, 2H, J = 1.9 Hz, tpy), 8.18 (s, 2H, tpy), 8.44 (d, 2H, J = 1.9 Hz, 3- and 3′-bipyridyl H's), 8.48 (d, 2H, J = 5.9 Hz, tpy), 8.93 (d, 2H, J = 5.9 Hz, 6- and 6′-bipyridyl H's). Positive FAB-MS: ion clusters at *m/z* 1184 {M}$^+$, 1156 {M − CO}$^+$. IR (KBr disk, ν/cm^{-1}): 1890 (s), 1908 (s), 1992 (s) ν(C≡O); 2012 (s), 2129 (m) ν(C≡C). Anal. Found (%): C 46.94, H 4.40, N 5.09. Calcd for [(^{t}Bu_2bpy)$(CO)_3$Re(C≡C−C≡C)Pt(^{t}Bu_3tpy)]OTf·$^1/_2CH_2Cl_2$: C 46.74, H 4.40, N 5.09.

Physical Measurements and Instrumentation. UV−visible spectra were obtained on a Hewlett-Packard 8452A diode array spectrophotometer, IR spectra as KBr disk on a Bio-Rad FTS-7 Fourier transform infrared spectrophotometer (4000−400 cm^{-1}), and steady-state excitation and emission spectra on a Spex Fluorolog-2 Model F 111 fluorescence spectrofluorometer equipped with a Hamamatsu R-928 photomultiplier tube. Low-temperature (77 K) spectra were recorded by using an optical Dewar sample holder. ^{1}H NMR spectra were recorded on a Bruker DPX-300 (300 MHz) Fourier transform NMR spectrometer with chemical shifts recorded relative to tetramethylsilane (Me_4Si). Positive-ion FAB mass spectra were recorded on a Finnigan MAT95 mass spectrometer. Elemental analyses for the metal complexes were performed on the Carlo Erba 1106 elemental analyzer at the Institute of Chemistry, Chinese Academy of Sciences, Beijing, China.

Emission lifetime measurements were performed using a conventional laser system. The excitation source was the 355 nm output (third harmonic) of a Spectra-Physics Quanta-Ray Q-switched GCR-150 pulsed Nd:YAG laser (10 Hz). Luminescence decay signals were recorded on a Tektronix Model TDS-620A (500 MHz, 2GS/s) digital oscilloscope and analyzed using a program for exponential fits. All solutions for photophysical studies were degassed on a high-vacuum line in a two-compartment cell consisting of a 10 mL Pyrex bulb and a 1 cm path length quartz cuvette and sealed from the atmosphere by a Bibby Rotaflo HP6 Teflon stopper. The solutions were subject to at least four freeze−pump−thaw cycles.

Cyclic voltammetric measurements were performed by using a CH Instruments, Inc. Model CHI 750A electrochemical analyzer interfaced to a personal computer. The electrolytic cell used was a conventional two-compartment cell. The reference electrode was separated from the working electrode compartment by a Vycor glass. A Ag/$AgNO_3$ (0.1 M in MeCN) reference electrode was used. The ferrocenium−ferrocene couple was used as the internal standard in the electrochemical measurements in acetonitrile (0.1 M ^{n}Bu_4NPF_6).[11] The working electrode was a glassy carbon (Atomergic Chemetals V25) electrode with a platinum gauze acting as the counter electrode.

The EHMO calculations were carried out using the standard extended Hückel method[12] with the CACAO program (Version 5.0).[12b] Standard atomic parameters were taken for H, C, O, and N.[12c] The exponents (ζ) and the valence shell ionization potential (H_{ii} in eV) used for Re and Pt were the standard CAChe parameters,[13] i.e., 2.398 and 9.360 for 6s (Re), 2.372 and 5.960 for 6p (Re), 2.554 and 9.080 for 6s (Pt), and 2.554 and 5.470 for 6p (Pt), respectively. The H_{ii} values for 5d Re and Pt were 12.660 and 12.590, respectively. A linear combination of two Slater-type orbitals (Re: ζ_1 = 5.343, c_1 = 0.6662, ζ_2 = 2.277, c_2 = 0.5910; Pt: ζ_1 = 6.013, c_1 = 0.6334, ζ_2 = 2.696, c_2 = 0.5513) was used to represent the atomic 5d orbitals.

Crystal Structure Determination. Single crystals of **1** were obtained by recrystallization from dichloromethane−*n*-hexane. A red crystal of dimensions 0.50 × 0.20 × 0.10 mm mounted on a glass fiber was used for data collection at −20 °C on a MAR diffractometer with graphite-monochromatized Mo Kα radiation (λ = 0.71073 Å). The images were interpreted and intensities integrated using the program DENZO.[14] A total of 13 348 reflections were measured, of which 8412 were unique (R_{int} = 0.0372) and were used in all calculations, 5015 reflections with $F > 4\sigma(F_o)$. The structure was solved by direct methods employing the SIR-97 program[15] on a PC and refinement by full-matrix least-squares using the software package SHELXL-97[16] on a PC. One crystallographic asymmetric unit consists of half of a formula unit, including one triflate anion and three dichloromethane molecules. In the least-squares refinement, O, F, and C atoms of the anion and non-hydrogen atoms of solvent molecules were refined isotropically; other non-hydrogen atoms were refined anisotropically. H atoms were generated by the program SHELXL-97.[16] Convergence for 614 variable parameters by full-matrix least-squares refinement on F^2 with $(\Delta/\sigma)_{max}$ = 0.001 (av 0.001) was reached at R_1 = 0.0665 ($I > 2\sigma(I)$) and wR_2 = 0.1922 with a goodness-of-fit of 0.991. Single crystals of **4** were obtained by recrystal-

(11) Gagne, R. R.; Koval, C. A.; Lisensky, G. C. *Inorg. Chem.* **1980**, *19*, 2854.

(12) (a) Hoffmann, R.; Lipscomb, W. N. *J. Chem. Phys.* **1962**, *36*, 2179. (b) Mealli, C.; Proserpio, D. M. *J. Chem. Educ.* **1990**, *67*, 399. (c) Hoffmann, R. *J. Chem. Phys.* **1963**, *39*, 1397.

(13) Dedieu, A.; Albright, T. A.; Hoffmann, R. *J. Am. Chem. Soc.* **1979**, *101*, 3141.

(14) Otwinowski, Z.; Minor, W. In *Methods in Enzymology*, *Vol. 276*: *Macromolecular Crystallography, part A*; Carter, C. W., Sweet, R. M., Jr., Eds.; Academic Press: New York, 1997; pp 307−326.

(15) Altomare, A.; Burla, M. C.; Camalli, M.; Cascarano, G.; Giacovazzo, C.; Guagliardi, A.; Moliterni, A. G. G.; Polidori, G.; Spagna, R. *Sir97*: A new tool for crystal structure determination and refinement. *J. Appl. Crystallogr.* **1998**, *32*, 115.

(16) Sheldrick, G. M. *SHELXL97*, Programs for Crystal Structure; University of Göttingen: Germany, 1997.

Table 1. Crystal and Structure Determination Data for Complexes 1 and 4

	1	4
empirical formula	$[C_{51}H_{47}F_3N_5O_6PtReS\cdot 3CH_2Cl_2]$	$[C_{53}H_{46}F_3N_6O_8PtReS\cdot 2CH_3CN]$
M_r	1551.06	1447.42
cryst syst	triclinic	monoclinic
space group	$P\bar{1}$ (No. 2)	$P2_1/n$ (No. 14)
a/Å	10.676(2)	15.738(3)
b/Å	17.232(3)	14.944(3)
c/Å	20.341(4)	28.052(6)
α/deg	65.50(3)	90
β/deg	87.08(3)	102.89(3)
γ/deg	72.11(3)	90
V/Å^3	3227.9(10)	6431(2)
Z	2	4
μ(Mo Kα) (cm^{-1})	43.74	41.48
T/K	253(2)	253(2)
λ/Å (graphite monochromated, Mo Kα)	0.71073	0.71073
no. of reflns collected	13 348	32 682
no. of indep reflns	8412 [$R_{int} = 0.0372$]	10 543 [$R_{int} = 0.0795$]
final R indices [$I > 2\sigma(I)$]	$R_1 = 0.0665$, $wR_2 = 0.1922^a$	$R_1 = 0.0445$, $wR_2 = 0.1058^a$
R indices (all data)	$R_1 = 0.1014$, $wR_2 = 0.2129^a$	$R_1 = 0.0757$, $wR_2 = 0.1104^a$
weighting scheme	$a = 1.3348$, $b = 0$	$a = 0.0120$, $b = 0$
goodness-of-fit on F^2	0.991	0.865
largest diff peak and hole, e Å^{-3}	2.253 and −1.816	0.966 and −1.127

^{a} $wR_2 = \{\sum[w(F_o^2-F_c^2)^2]/\sum[w(F_o^2)^2]\}^{1/2}$; $w = 1/[\sigma^2(F_o^2) + (aP) + bP]$, where $P = [2F_c^2 + \mathrm{Max}(F_o^2,0)]/3$.

lization from diffusion of diethyl ether vapor into an acetonitrile solution of **4**. A red crystal of dimensions 0.45 × 0.40 × 0.05 mm mounted on a glass fiber was used for data collection at −20 °C on a MAR diffractometer with graphite-monochromatized Mo Kα radiation (λ = 0.71073 Å). The images were interpreted and intensities integrated using the program DENZO.[14] A total of 32 682 reflections were measured, of which 10 543 were unique (R_{int} = 0.0795) and were used in all calculations, 5919 reflections with $F > 4\sigma(F_0)$. The structure was solved by direct methods employing the SIR-97 program[15] on a PC and refinement by full-matrix least-squares using the software package SHELXL-97[16] on a PC. One crystallographic asymmetric unit consists of one formula unit. The NO_2− group was disordered into two neighboring positions. In the least-squares refinement, disordered atoms (except sulfur) and three carbon atoms of one *tert*-butyl group were refined isotropically; other non-hydrogen atoms were refined anisotropically. H atoms (except those on acetonitrile) were generated by the program SHELXL-97.[16] Convergence for 663 variable parameters by full-matrix least-squares refinement on F^2 with $(\Delta/\sigma)_{max} = 0.001$ (av 0.001) was reached at $R_1 = 0.0445$ ($I > 2\sigma(I)$) and $wR_2 = 0.1058$ with a goodness-of-fit of 0.865. Crystal and structure determination data for **1** and **4** are summarized in Table 1. The final agreement factors for **1** and **4** are given in Table 1. Selected bond distances and angles are summarized in Table 2.

Results and Discussion

Synthesis and Characterization. Preparation of complexes **1**−**6** was accomplished by adding a DMF solution of [Re(N^N)(CO)$_3${C≡C−(C$_6$H$_4$)$_n$−C≡CH}] to a DMF solution of [Pt(N^N^N)Cl]OTf, CuI, and Et$_3$N under an inert atmosphere of nitrogen at room temperature. The reaction mixture was allowed to stir for 24 h. Precipitation of the crude product as a red solid was accomplished by addition of diethyl ether to the reaction mixture, followed by purification by column chromatography and subsequent recrystallization from acetonitrile−diethyl ether or dichloromethane−diethyl ether to afford the product as deep red crystals. Complexes **1**−**6** gave satisfactory elemental analysis and have been characterized by ^{1}H NMR, IR, and positive FAB-MS. The X-ray crystal structures of **1** and **4** have also been determined.

Table 2. Selected Bond Distances (Å) and Bond Angles (deg) for 1 and 4, with Estimated Standard Deviations Given in Parentheses

		1	
Pt(1)−N(1)	2.029(13)	Pt(1)−N(2)	1.958(12)
Pt(1)−N(3)	2.015(13)	Pt(1)−C(28)	2.04(2)
C(28)−C(29)	1.19(2)	C(36)−C(37)	1.19(2)
Re(1)−C(37)	2.096(17)	Re(1)−N(4)	2.155(13)
Re(1)−N(5)	2.190(15)	Re(1)−C(38)	1.90(2)
Re(1)−C(39)	1.86(2)	Re(1)−C(40)	1.85(2)
N(1)−Pt(1)−N(2)	80.3(5)	N(1)−Pt(1)−N(3)	160.5(5)
C(29)−C(28)−Pt(1)	179.5(17)	C(36)−C(37)−Re(1)	176.5(15)
C(38)−Re(1)−C(37)	177.0(7)	N(4)−Re(1)−N(5)	74.7(5)
		4	
Pt(1)−N(4)	1.972(8)	Pt(1)−N(5)	1.974(6)
Pt(1)−N(6)	1.994(8)	Pt(1)−C(25)	1.982(8)
C(24)−C(25)	1.186(10)	C(16)−C(17)	1.195(10)
Re(1)−C(16)	2.140(8)	Re(1)−N(1)	2.183(7)
Re(1)−N(2)	2.161(8)	Re(1)−C(1)	1.924(8)
Re(1)−C(2)	1.842(11)	Re(1)−C(3)	1.747(14)
N(4)−Pt(1)−N(5)	80.1(3)	N(4)−Pt(1)−N(6)	160.9(3)
C(24)−C(25)−Pt(1)	177.9(9)	C(17)−C(16)−Re(1)	174.8(8)
C(1)−Re(1)−C(16)	178.6(4)	N(1)−Re(1)−N(2)	75.1(3)

Crystal Structure Determination. Figures 1 and 2 depict the perspective drawings of the complex cations of **1** and **4** with atomic numbering, respectively. Both structures show a slightly distorted octahedral coordination geometry about rhenium, with the three carbonyl ligands arranged in a facial fashion. The N−Re−N angles of less than 90° are observed (74.7(5)° for **1** and 75.1(3)° for **4**), as required by the bite distance exerted by the steric demand of the chelating bipyridine and phenanthroline ligands. The coordination geometry about the platinum center is distorted square planar, with the N−Pt−N angles deviated from the idealized values of 90° and 180°. Such distortion is clearly the consequence of the steric demand of the terpyridine ligand. The bond length of the C≡C bond that is bonded

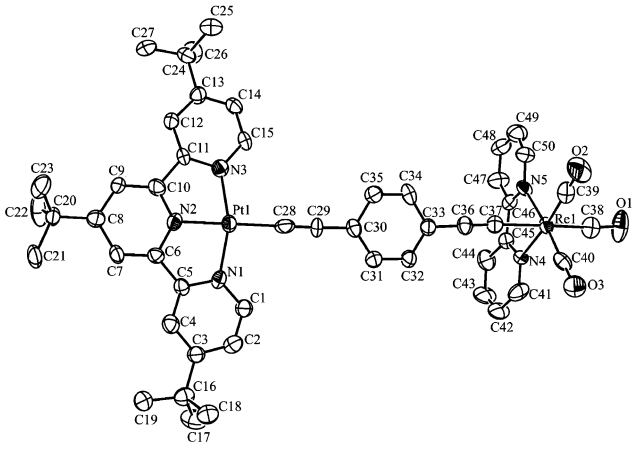

Figure 1. Perspective drawing of the complex cation of **1** with atomic numbering scheme. All hydrogen atoms, solvent molecules, and triflate anion have been omitted for clarity. Thermal ellipsoids are shown at the 30% probability level.

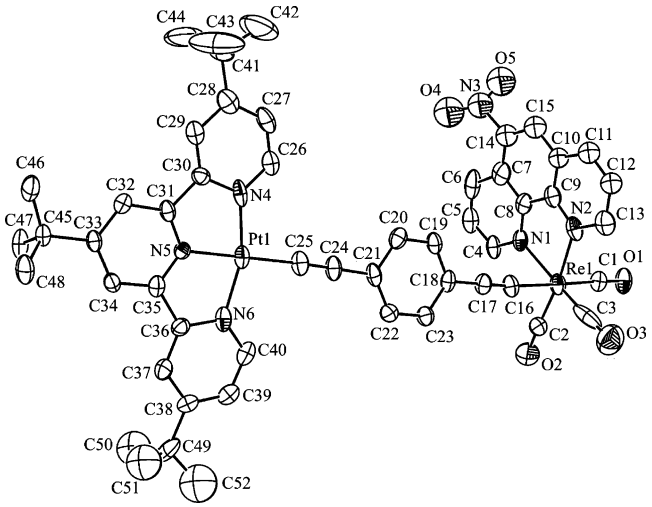

Figure 2. Perspective drawing of the complex cation of **4** with atomic numbering scheme. All hydrogen atoms, solvent molecules, and triflate anion have been omitted for clarity. Thermal ellipsoids are shown at the 30% probability level.

to Re is 1.19(2) Å for **1** and 1.195(10) Å for **4**, while the one bonded to Pt is 1.19(2) Å for **1** and 1.186(10) Å for **4**, which are comparable to those of other Re(I) and Pt(II) alkynyl systems.[5,6] The Re−C≡C and Pt−C≡C units are essentially linear with a Re−C≡C bond angle of 176.5(15)° and 174.8(8)° and a Pt−C≡C bond angle of 179.5(17)° and 177.9(9)° for **1** and **4**, respectively, similar to those found in other related Re(I) and Pt(II) alkynyl systems.[5,6]

Electronic Absorption and Emission. The electronic absorption spectra of **1**−**6** in acetonitrile show, in addition to the high-energy absorptions at ca. 288−378 nm, typical of $\pi \rightarrow \pi^*$ intraligand transitions of bipyridine, terpyridine, and the alkynyl ligands, two intense absorption bands at ca. 404−486 nm, with extinction coefficients on the order of 10^3 dm^3 mol^{-1} cm^{-1}. Table 3 summarizes the electronic absorption data of the complexes. With reference to the electronic absorption studies of platinum(II) terpyridine alkynyl[6] and rhenium(I) diimine alkynyl[5] systems, the low-energy absorptions are tentatively assigned as admixtures of [dπ(Pt) $\rightarrow$ π^*(N^N^N)] MLCT, [dπ(Re) $\rightarrow$ π^*(N^N)] MLCT, and [π(C≡C−R) $\rightarrow$ π^*(N^N^N) or π^*-(N^N)] ligand-to-ligand charge transfer (LLCT) transitions since both the platinum terpyridyl and rhenium diimine systems absorb at similar energies. The lower absorption energy of the low-energy absorption band of **5** (486 nm) than **2** (468 nm) and the relative insensitivity of the energy of this low-energy band among **1**−**4** are in line with the higher π^* orbital energy of ^{t}Bu$_3$tpy than tpy as a result of the poorer π-accepting ability of ^{t}Bu$_3$-tpy derived from the presence of the more electron-rich *tert*-butyl substituents on the terpyridine ligand. This is also suggestive of the dominating [dπ(Pt) $\rightarrow$$\pi^*$-(N^N^N)] MLCT and [$\pi$(C≡C−R) $\rightarrow$ π^*(N^N^N)] LLCT character in this low-energy transition band.

Upon photoexcitation of **1**−**6** at $\lambda > 380$ nm, intense orange-red luminescence was observed both in the solid state and in fluid solutions at room temperature (Table 3). With the same *tert*-butyl-substituted terpyridine ligand, complexes **1**−**4** show similar emission energies irrespective of the nature of the substituents on the diimine ligand of the [Re(CO)$_3$(N^N)] moiety. Such observation is different from those rhenium mixed-metal complexes that we previously reported.[7] The emission energies are also found to be fairly similar to that of the platinum alkynyl precursor, [Pt(^{t}Bu$_3$tpy)(C≡C−C$_6$H$_4$−C≡C−H)]OTf (581 nm). Complex **5**, with an unsubstituted terpyridyl ligand, is found to exhibit a lower emission energy (608 nm) than that of **2** (580 nm), consistent with the lower π^* orbital energy of tpy than ^{t}Bu$_3$tpy as a result of its better π-accepting ability derived from the absence of the more electron-rich *tert*-butyl substituents on the terpyridine ligand. Thus the emission of this class of complexes is attributed to be derived from an excited state of [dπ(Pt) $\rightarrow$ π^*(N^N^N)] ^{3}MLCT origin that has been modified by the rhenium diimine alkynyl moiety and probably mixed with some [π(C≡C−R) $\rightarrow$ π^*(N^N^N)] LLCT character,[6g] or alternatively of [π(C≡C−(C$_6$H$_4$)$_n$C≡C−[Re]) $\rightarrow$ π^*(N^N^N)] metalloligand-to-ligand charge transfer origin. One might expect at first sight that the lowest energy emission would be derived mainly from the rhenium diimine moiety, based on the fact that the rhenium(I) alkynyl precursors exhibit lower emission energy (ca. 610 nm) than that of the platinum(II) alkynyl precursors (ca. 580 nm). However, the rhenium(I) diimine excited state energy is in fact not the lowest in the heterobimetallic system. This is because the dπ(Re) orbital energy actually would be lowered upon coordination of a cationic platinum terpyridyl unit, resulting from the poorer donating abilities of the alkynyl ligand. On the contrary, this effect on the platinum moiety is relatively less significant since the rhenium moiety is neutral. On the other hand, variation of the alkynyl bridge has also been observed to affect the emission energy. It is found that **6** (570 nm) exhibits a slightly higher emission energy than **2** (580 nm) (Figure 3), which may be attributed to the poorer π-donating ability of C≡C−C≡C than C≡C−C$_6$H$_4$−C≡C,[17] rendering the Pt(II) center less electron-rich and lowering the dπ orbital energy of platinum in **6**. The unexpected localization of the lowest-energy emissive state on the platinum(II) terpyridyl moiety in these mixed-metal alkynyl-bridged molecular rods represents an interesting phenomenon brought about by the linking together of the two MLCT luminophores.

Electrochemical Properties. The cyclic voltammograms of **1**−**6** in acetonitrile (0.1 mol dm^{-3} ^{n}Bu$_4$NPF$_6$) display two irreversible oxidation waves at ca. +1.0 and +1.4 V, respectively, a quasi-reversible oxidation couple at ca. +1.9 V, and two quasi-reversible reduction couples at ca. −1.0 and −1.5 V vs SCE, respectively. The electrochemical data are summarized in Table 4. The representative cyclic voltammograms of **2** and **5** are shown in Figure 4. The first irreversible oxidation wave at ca. +1.0 V vs SCE may be tentatively assigned as the oxidation of the alkynyl ligand, based on electrochemical studies on the 1,4-diethynylbenzene (+1.21 V vs SCE); however, possible involvement of Re(I) oxidation cannot be completely excluded. Another irreversible oxidation wave at ca. +1.4 V vs SCE was attributed to a metal-centered oxidation from Pt(II) to Pt(III).

(17) (a) Sonogashira, K.; Fujikura, Y.; Yatake, T.; Toyoshima, N.; Takahashi, S.; Hagihara, N. *J. Organomet. Chem.* **1978**, *145*, 101. (b) Biswas, M.; Nguyen, P.; Marder, T. B.; Khundkar, L. R. *J. Phys. Chem. A* **1997**, *101*, 1689.

Table 3. Electronic Absorption and Emission Data for 1−6

		emission	
complex	electronic absorption λ_{max}/nm (ϵ/dm^3 mol^{-1} cm^{-1})[a]	medium (T/K)	λ_{em}/nm (τ_o[b]/μs)
1	290 (79860), 326 (51105), 404 (8360), 470 (8870)	MeCN (298)	580 (0.61)
		solid (298)	688 (0.13)
		solid (77)	662 (1.50)
		EtOH−MeOH glass (4:1 v/v) (77)	604 (8.70, 2.04)[c]
2	296 (71170), 328 (55265), 402 (8550), 468 (8330)	MeCN (298)	580 (0.69)
		solid (298)	685 (0.25)
		solid (77)	677 (0.92)
		EtOH−MeOH glass (4:1 v/v) (77)	614 (9.27, 2.06)[c]
3	290 (71740), 324 (60390), 404 (7625), 470 (9955)	MeCN (298)	580 (0.89)
		solid (298)	651 (0.26)
		solid (77)	628 (1.03)
		EtOH−MeOH glass (4:1 v/v) (77)	625 (2.48)
4	288 (58370), 328 (51835), 406 (7305), 468 (8470)	MeCN (298)	575 (0.94)
		solid (298)	621 (0.12)
		solid (77)	660 (0.87)
		EtOH−MeOH glass (4:1 v/v) (77)	615 (2.87)
5	294 (69020), 330 (49070), 406 (8290), 486 (7755)	MeCN (298)	608 (0.65)
		solid (298)	nonemissive
		solid (77)	nonemissive
		EtOH−MeOH glass (4:1 v/v) (77)	622 (3.94)
6	298 (42625), 324 (24395), 378 (5200), 404 sh (5380), 484 (8585)	MeCN (298)	570 (0.52)
		Solid (298)	733 (0.23)
		solid (77)	697 (0.41)
		EtOH−MeOH glass (4:1 v/v) (77)	638 (1.04)

[a] In MeCN at 298 K. [b] Recorded with an uncertainty of ±10%. [c] Double exponential decay.

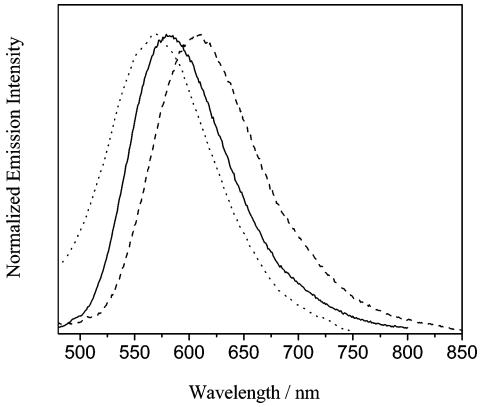

Figure 3. Normalized emission spectra of **2** (—), **5** (- - -), and **6** (····) in degassed MeCN at 298 K.

Table 4. Electrochemical Data for 1−6

complex	oxidation[a] $E_{1/2}$[b]/V vs SCE (ΔE_p/mV)	reduction[a] $E_{1/2}$[b]/V vs SCE (ΔE_p/mV)
1	+0.96[c], +1.38[c], +1.90 (96)	−1.01 (48), −1.48 (87)
2	+0.94[c], +1.36[c], +1.86 (90)	−1.01 (85), −1.51 (88)
3	+1.06[c], +1.40[c], +1.96 (90)	−1.01 (72), −1.51 (63)
4	+1.02[c], +1.42[c], +2.00 (96)	−1.02 (84), −1.51 (89)
5	+0.94[c], +1.41[c], +1.86 (94)	−0.90 (69), −1.37 (90)
6	+0.95[c], +1.35[c], +1.85 (87)	−1.02 (55), −1.52 (94)

[a] In acetonitrile (0.1 mol dm^{-3} ^{n}Bu$_4$NPF$_6$). Working electrode: glassy carbon; ΔE_p of Fc$^+$/Fc ranges from 62 to 64 mV; scan rate, 100 mV s^{-1}. [b] $E_{1/2} = (E_{pa} + E_{pc})/2$; E_{pa} and E_{pc} are the anodic and cathodic peak potentials, respectively. $\Delta E_p = |E_{pa} - E_{pc}|$. [c] Irreversible oxidation wave. The potential refers to E_{pa}, which is the anodic peak potential.

Similar results were reported in the platinum(II) terpyridyl alkynyl complexes.[6]

In addition, the quasi-reversible oxidation couple at ca. +1.9 V vs SCE was found to vary significantly with the nature of the diimine ligand. This, together with the similarity of the potential for the oxidation of Re(I) to Re(II) in [Re(CO)$_3$(N^N)(MeCN)]$^+$,[5b,e,g,18] suggested

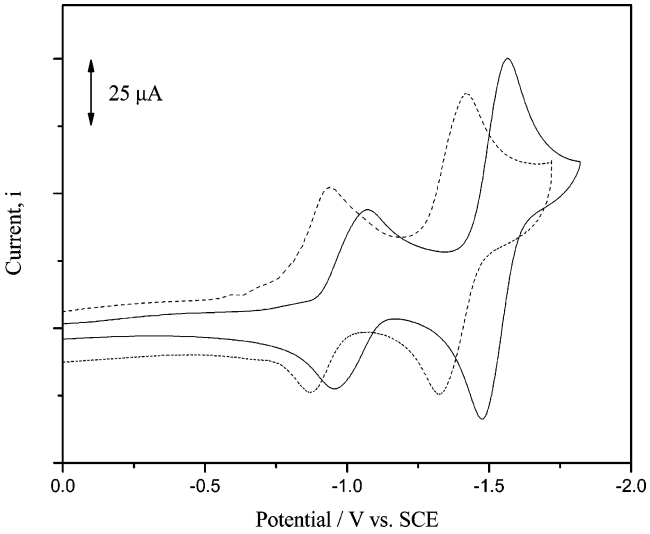

Figure 4. Cyclic voltammograms showing the reduction of **2** (—) and **5** (- - -) in acetonitrile (0.1 mol dm^{-3} ^{n}Bu$_4$NPF$_6$).

that the oxidation couple was a result of an EC mechanism that gave rise to the corresponding solvento complex, [Re(CO)$_3$(N^N)(MeCN)]$^+$, in acetonitrile. Slightly less positive potential values of +1.86 V in **2**, +1.86 V in **5**, and +1.85 V in **6** vs SCE than **1** (+1.90 V vs SCE) were observed, in line with the presence of the more electron-rich and less π-accepting ^{t}Bu$_2$bpy ligand that would make the Re(I) center in [Re(CO)$_3$(^{t}Bu$_2$bpy)(MeCN)]$^+$ more easily oxidized than that in [Re(CO)$_3$(bpy)(MeCN)]$^+$. Using similar arguments, the more positive potentials of **3** (+1.96 V vs SCE) and **4** (+2.00 V vs SCE) than **1** are attributed to the electron-withdrawing effects of the substituents on the (CF$_3$)$_2$-bpy and NO$_2$phen ligands, respectively.

On the other hand, the two quasi-reversible reduction couples at ca. −1.0 and −1.5 V vs SCE in the cyclic voltammograms of **1**−**6** were ascribed to the successive

Table 5. Calculated Molecular Orbital Energies and Transition Energies of 1 and 4

complex	molecular orbital no.	level/eV	composition/%						HOMO−LUMO energy gap, ΔE_{gap}/eV
			Pt	^{t}Bu$_3$tpy	Re	C≡C−C$_6$H$_4$−C≡C	bpy	CO	
1	142	−9.385	2	81	- -[a]	- -[a]	- -[a]	- -[a]	2.016
	143	−9.438	- -[a]	- -[a]	- -[a]	- -[a]	90	2	(145 → 144)
	144 (LUMO)	−9.860	4	78	- -[a]	- -[a]	- -[a]	- -[a]	
	145 (HOMO)	−11.876	49	2	- -[a]	17	- -[a]	- -[a]	
	146	−11.918	34	- -[a]	- -[a]	43	- -[a]	- -[a]	
	147	−12.118	65	15	- -[a]	- -[a]	- -[a]	- -[a]	
			Pt	^{t}Bu$_3$tpy	Re	C≡C−C$_6$H$_4$−C≡C	NO_2-phen	CO	
4	149	−9.655	- -[a]	- -[a]	- -[a]	- -[a]	84	- -[a]	2.071
	150	−9.746	4	70	- -[a]	- -[a]	- -[a]	- -[a]	(152 → 151)
	151 (LUMO)	−9.795	- -[a]	- -[a]	- -[a]	- -[a]	84	- -[a]	
	152 (HOMO)	−11.866	60	4	- -[a]	12	- -[a]	- -[a]	
	153	−11.950	29	- -[a]	- -[a]	46	- -[a]	- -[a]	
	154	−12.027	- -[a]	- -[a]	- -[a]	- -[a]	82	- -[a]	

[a] Percentage composition of less than 0.5%.

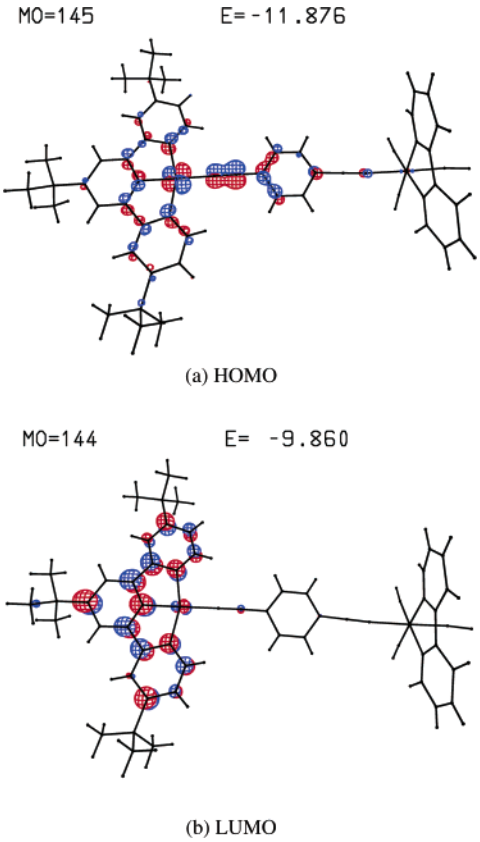

Figure 5. CACAO plots of (a) HOMO and (b) LUMO of **1**.

ligand-centered reductions of the terpyridine ligand, similar to that observed in other platinum(II) terpyridyl systems.[6a] It is noted that **5** (−0.90 and −1.37 V vs SCE) showed less negative reduction potentials than that for the other complexes due to the absence of *tert*-butyl groups on the terpyridine ligand, which would increase the ease of reduction.

EHMO Calculations. The molecular orbital studies of complexes **1** and **4** have been performed by extended Hückel molecular orbital (EHMO) theory. Table 5 summarizes the calculated molecular orbital energies, percentage composition, and the HOMO−LUMO energy gap. Complex **1** shows that the LUMO mainly consists of π^*(^{t}Bu$_3$tpy) character, while the HOMO is mainly dominated by the antibonding character of the [Pt(C≡C−C$_6$H$_4$−C≡C)] moiety resulting from the overlap of the dπ(Pt) and π(C≡C−C$_6$H$_4$−C≡C) orbitals (Figure 5). Such filled−filled dπ−pπ interactions have also been reported.[19] For complex **4**, although the LUMO was dominated by the π^*(NO_2phen) character, the relatively

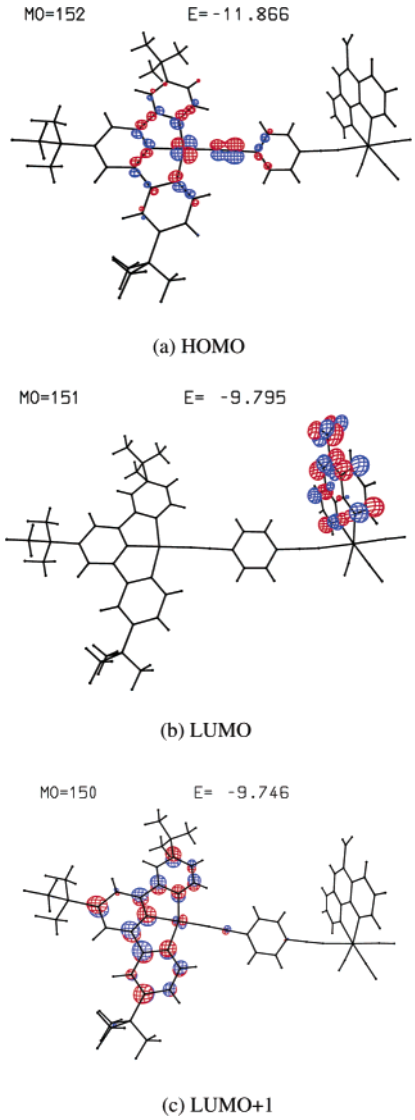

Figure 6. CACAO plots of (a) HOMO, (b) LUMO, and (c) LUMO+1 of **4**.

small energy difference between the LUMO and LUMO+1 would suggest that the LUMO would consist of admixtures of $\pi^*(NO_2phen)$ and $\pi^*(^tBu_3tpy)$ characters, whereas the HOMO is again mainly dominated by the antibonding character of the $d\pi(Pt)$ and $\pi(C{\equiv}C{-}C_6H_4{-}C{\equiv}C)$ orbital overlap (Figure 6). These results are supportive of an assignment of a mixed $[d\pi(Pt) \rightarrow \pi^*(N\text{^}N\text{^}N)]$ MLCT/$[\pi(C{\equiv}C{-}R) \rightarrow \pi^*(N\text{^}N\text{^}N)]$ LLCT character for the electronic transition, probably with some mixing of a charge transfer character to the bipyridyl or phenanthroline moiety in the case of the presence of electron-deficient π-acceptors such as NO_2phen in **4**. This further supports the electrochemical studies, in which the first and second oxidation waves were ascribed to alkynyl ligand-centered and platinum(II) metal-centered oxidations. The first reduction couples, on the other hand, were assigned as the one-electron terpyridine ligand-centered reductions.

Conclusion

A new class of luminescent heterometallic rhenium(I)−platinum(II) polypyridine alkynyl complexes has been successfully synthesized and characterized; the X-ray crystal structures of **1** and **4** have also been determined. The emission origin was assigned as derived from excited states of $[d\pi(Pt) \rightarrow \pi^*(N\text{^}N\text{^}N)]$ ^{3}MLCT origin modified by the rhenium diimine alkynyl moiety and probably mixed with some $[\pi(C{\equiv}C{-}R) \rightarrow \pi^*(N\text{^}N\text{^}N)]$ LLCT character, or alternatively of $[\pi(C{\equiv}C{-}(C_6H_4)_nC{\equiv}C{-}[Re]) \rightarrow \pi^*(N\text{^}N\text{^}N)]$ metalloligand-to-ligand charge transfer origin. The unexpected localization of the lowest-energy emissive state on the platinum(II) terpyridyl moiety in these heterometallic bichromophoric systems is further supported by electrochemical studies and the extended Hückel molecular orbital (EHMO) calculations.

Acknowledgment. V.W.W.Y. acknowledges financial support from the University Development Fund of The University of Hong Kong, The University of Hong Kong Foundation for Education Development and Research Limited, and the Research Grants Council of the Hong Kong Special Administrative Region, China (Project No. HKU 7022/03P). S.C.F.L. acknowledges the receipt of a postgraduate studentship, a Li Po Chun Scholarship, and Sir Edward Youde Memorial Fellowship, administered by The University of Hong Kong, the Li Po Chun Charitable Fund, and Sir Edward Youde Memorial Fund Council, respectively. The award of a grant by the CNRS/RGC under the PROCORE: France-Hong Kong Joint Research Scheme (F-HK 33/04T) is gratefully acknowledged.

Supporting Information Available: Crystallographic data for complexes **1** and **4** are given as CIF files. This material is available free of charge via the Internet at http://pubs.acs.org.

OM0502887

(18) Caspar, J. V.; Meyer, T. J. *J. Phys. Chem.* **1983**, *87*, 952.
(19) Lichtenberger, D. L.; Renshaw, S. K.; Bullock, R. M. *J. Am. Chem. Soc.* **1993**, *115*, 3276.